it is concluded that failure to observe these must be due to the necessity of substantial molecular rearrangement to facilitate the formation of an H_2O bound in an appropriate configuration for loss. Evidently energy dissipation through CH_3OH loss is much more facile and is the dominant channel at intermediate cluster sizes; in fact, it is the only channel observed for the protonated trimer.

In addition to the evaporative loss of methanol, and the reaction of the protonated dimer which leads to the production of protonated dimethyl ether and elimination of water, several other size-dependent intracluster reaction pathways have been revealed in the present study. In the case of intermediate and larger clusters, $(CH_3)_2O$ (along with CH_3OH) is lost while H_2O is retained by the cluster. For clusters comprised of four to nine methanol molecules, the $(CH_3)_2O$ elimination is observed to occur over the time window 1 to 15 μs after ionization as evidenced by the observed mass loss during flight through the field-free region to the reflectron.

For larger clusters, the appearance of $H^+(H_2O)(CH_3OH)_n$ in the conventional TOF mass spectrum implies that the elimination takes place well before the ions enter the field-free region. The loss of $(CH_3)_2O$ occurs on a rapid time scale (in the ion lens) creating mixed clusters of form $H^+{\cdot}H_2O(CH_3OH)_n$ where n = 7 or greater (**b** peaks, Figure 2). An ion with the mass of $H^+(CH_3OH)_7$ requires about 1.3 μs to exit the acceleration field and enter the field-free region under the experimental conditions employed in the experiments.

The results can be explained by estimates that ether is only slightly more strongly bound than methanol to protonated methanol clusters of size n = 4, and the solvation may be about thermoneutral at n = 5. Beyond this size the solvation of CH_3OH may be preferential. The reason why $(CH_3)_2O$ elimination is accompanied by CH_3OH loss is not clear. It may be that the excess energy of the rearrangement is accommodated through evaporative methanol loss.

Based on high-pressure mass spectrometric measurements of mixed protonated alcohol–water clusters comprised of all combinations up to a total of six molecules, Kebarle and co-workers[10] concluded that in small ion clusters methanol is preferentially solvated by the proton, while in ones with more than a total of nine molecules, interaction with water would dominate over that of methanol. It is worth noting that these findings are in general accord with the results of Stace and Shukla[13] who present fragmentation results for mixed water–methanol cluster studies which display a reversal in the trend of water and methanol loss with cluster size from preformed mixed cluster systems. In view of an expected switch-over in relative solvation, our findings of the appearance of a protonated water cluster bound with methanol molecules beginning at size n = 7 is consistent with these findings.

Acknowledgment. Financial support by the U.S. Department of Energy, Grant DE-ACO2-82ER60055, is gratefully acknowledged and the Army Research Office, Grant No. DAAG29-85-K0215.

Registry No. CH_3OH, 67-56-1.

Periodic Trends in Chemical Reactivity: Reactions of Sc^+, Y^+, La^+, and Lu^+ with Methane and Ethane

L. S. Sunderlin[†] and P. B. Armentrout*[,‡,§]

Contribution from the Departments of Chemistry, University of California, Berkeley, California 94720, and University of Utah, Salt Lake City, Utah 84112.
Received September 19, 1988

Abstract: The reactions of Sc^+, Y^+, La^+, and Lu^+ with methane and ethane are examined using guided ion beam mass spectrometry. With methane, the major products are MCH_2^+ at low energy and MH^+ at high energy, with small amounts of MCH_3^+ also seen. The results for reaction of Y^+, La^+, and Lu^+ with ethane are similar to those reported previously for Sc^+. Single and double dehydrogenation are exothermic for Sc^+, Y^+, and La^+ but endothermic for Lu^+. MH_2^+ is formed in endothermic reactions at low energies for all four metals. At high energy, MH^+, MCH_2^+, and MCH_3^+ are the major products. A molecular orbital model previously used to explain the reactivity of metal ions with H_2 is extended to explain the reactivity seen here. The results are analyzed to give $D°(M^+–CH_2)$, $D°(M^+–CH_3)$, the two-ligand bond energy of $D°(M^+–H) + D°(HM^+–H)$, and limits on $D°(M^+–C_2H_4)$ and $D°(M^+–C_2H_2)$ for all four metals.

Extensive progress in understanding the gas-phase activation of carbon–hydrogen and carbon–carbon bonds by transition-metal ions has been made recently.[1,2] Such studies can provide quantitative thermochemistry[3] as well as insight into the periodic trends of reactivity.[1,4] Recent studies in our laboratories have shown that the reactions of atomic transition-metal ions with dihydrogen are sensitive to the electronic state and configuration of the metal ion and have formulated guidelines describing the reactivity seen.[4,5] A previous paper that covers the reaction of H_2 with Sc^+ and its isovalent analogues, Y^+, La^+, and Lu^+, completes the study of the first row of the transition metals and compares reactivity trends within a column of the periodic table.[6] The reactivity guidelines derived in the H_2 system have also been extended to the reactions of Ti^+,[7] V^+,[8] Cr^+,[9] and Fe^+[10] with methane. This paper is a continuation of our investigations of the periodic trends in the reactivity of transition-metal ions with

[†] University of California.
[‡] University of Utah.
[§] NSF Presidential Young Investigator 1984–1989; Alfred P. Sloan Fellow; Camille and Henry Dreyfus Teacher-Scholar, 1988–1993.

(1) Armentrout, P. B. *Gas Phase Inorganic Chemistry*. In Modern Inorganic Chemistry; Russell, D. H., Ed.; Plenum: New York, 1989.
(2) Allison, J. *Prog. Inorg. Chem.* **1986**, *34*, 627–676, and references therein.
(3) Armentrout, P. B.; Georgiadis, R. *Polyhedron* **1988**, *7*, 1573–1581.
(4) Elkind, J. L., Armentrout, P. B. *J. Phys. Chem.* **1987**, *91*, 2037–2045.
(5) Elkind, J. L.; Armentrout, P. B. *J. Phys. Chem.* **1985**, *89*, 5626–5636; **1986**, *90*, 5736–5745, 6576–6586; *J. Chem. Phys.* **1986**, *84*, 4862–4871; **1987**, *86*, 1868–1877; *Int. J. Mass Spectrom. Ion Processes* **1988**, *83*, 259–284.
(6) Elkind, J. L.; Sunderlin, L. S.; Armentrout, P. B. *J. Phys. Chem.*, in press.
(7) Sunderlin, L. S.; Armentrout, P. B. *J. Phys. Chem.* **1988**, *92*, 1209–1219.
(8) Aristov, N.; Armentrout, P. B. *J. Phys. Chem.* **1987**, *91*, 6178–6188.
(9) Georgiadis, R.; Armentrout, P. B. *J. Phys. Chem.* **1988**, *92*, 7060–7067.
(10) Schultz, R. H.; Elkind, J. L.; Armentrout, P. B. *J. Am. Chem. Soc.* **1988**, *110*, 411–423.

0002-7863/89/1511-3845$01.50/0

Table I. Electronic States of Sc^+, Y^+, La^+, and Lu^+

	state	electron config	energy,[a] eV	population,[b] %
Sc^+[c]	a^3D	4s3d	0.013	87.5
	a^1D	4s3d	0.315	6.4
	a^3F	$3d^2$	0.608	6.1
	b^1D	$3d^2$	1.357	<0.1
Y^+[d]	a^1S	$5s^2$	0.000	11.2
	a^3D	5s4d	0.148	80.5
	a^1D	5s4d	0.409	7.1
	a^3F	$4d^2$	1.045	1.2
	a^3P	$4d^2$	1.742	<0.1
La^+[e]	a^3F	$5d^2$	0.147	68.4
	a^1D	6s5d	0.173	12.6
	a^3D	6s5d	0.342	17.0
	a^3P	$5d^2$	0.738	1.4
	a^1S	$6s^2$	0.917	0.1
	a^1G	$5d^2$	0.927	0.5
	b^1D	$5d^2$	1.252	<0.1
Lu^+[e]	a^1S	$6s^2$	0.000	99.5
	a^3D	6s5d	1.628	0.5
	a^1D	6s5d	2.149	<0.1

[a] Energies are a statistical average over the J levels. [b] Maxwell–Boltzmann distribution at 2300 K. [c] Values are from: Sugar, J.; Corliss, C. *J. Phys. Chem. Ref. Data* **1980**, *9*, 473–511. [d] Moore, C. E. *Natl. Stand. Ref. Data Ser. (U.S. Natl. Bur. Stand.)* **1971**, *35*. [e] Reference 44.

methane and ethane both across the first row of the periodic table and down one of its columns. The detailed reactivity of Sc^+ with ethane has been previously reported.[11]

Although such comparative studies are necessary to determine periodic trends within groups, few such studies are available, due mostly to the lack of studies of the second- and third-row transition metals. The exothermic reactions of Sc^+,[11,12] Y^+,[13] and La^+[13] with alkanes larger than methane, however, have been previously reported. These reports indicate that the group 3 elements show unusual reactivity, including the formation of dialkyl products. Even though different electronic states are occupied in these ions (Table I), the reactivity of Sc^+, Y^+, and La^+ with large alkanes is similar. The lanthanide ion Gd^+, which has two valence electrons and a half-filled 4f shell, also reacts like these group 3 ions with large alkanes.[14] This indicates that the 4f electrons do not participate in the reactivity of these ions. On this basis, we expect that Lu^+, with two valence electrons and a full 4f shell, should also react similarly to the other group 3 elements. The reactions of Lu^+ are also of interest because of work on condensed-phase C–H bond activation of methane by Lu compounds;[15] Sc compounds have also been shown to activate C–H bonds.[16]

Experimental Section

A complete description of the apparatus and experimental procedures is given elsewhere.[17] Briefly, the apparatus comprises three differentially pumped vacuum chambers. In the first chamber, ions are produced as described below. The resulting ions are extracted, accelerated, and focused into a magnetic sector momentum analyzer for mass analysis. In the second vacuum chamber, the mass-selected ions are decelerated to a desired kinetic energy and focused into an octopole ion guide. Radio-frequency electric fields in the guide create a radial potential well that traps ions over the mass range studied. The velocity of the ions parallel to the axis of the guide is unchanged. The octopole passes through a static gas cell into which the reactant gas can be introduced. Pressures, which are measured by an MKS Baratron capacitance manometer, are maintained at a sufficiently low level (less than 0.2 mTorr) that multiple ion–molecule collisions are improbable. The octopole ion guide ensures efficient collection of all ionic products and transmitted reactant ions. Product ion losses due to dynamic effects are small.[17] High product collection gives better sensitivity, allowing cross sections as small as 10^{-19} cm^2 to be measured. Thus, use of the octopole provides much better precision in the crucial threshold region of the endothermic reactions, as well as the ability to accurately monitor minor products. The ions are extracted from the octopole and focused into the third vacuum chamber, which contains a quadrupole mass filter for product mass analysis. Ions are detected with a secondary electron scintillation ion detector and processed by pulse-counting techniques. The experiments are automated by use of a DEC MINC computer, which collects the ion signals at different masses as it increments the incident ion energy.

The absolute energy of the ions in the interaction region is measured by using the octopole as a retarding field analyzer. The behavior of the octopole as a retarding analyzer has been verified by time-of-flight measurements[17] and comparisons with theory.[17,18] Uncertainties in the absolute energy scale are ±0.05 eV lab. The fwhm of the energy distribution is independent of energy and is typically ≃0.6 eV lab.

Translational energies in the laboratory frame of reference are related to energies in the center of mass (CM) frame by $E(\mathrm{CM}) = E(\mathrm{lab})m/(M + m)$, where M and m are the masses of the incident ion and neutral reactant, respectively. The ^{45}Sc isotope (100% natural abundance), ^{89}Y isotope (100% natural abundance), ^{139}La isotope (99.9% natural abundence), and ^{175}Lu isotope (97.4% natural abundance) were used in these experiments. Below ~0.3 eV lab, the energies are corrected for truncation of the ion beam energy distribution as described previously.[17] The data obtained in this experiment are broadened by two effects: the ion energy spread and thermal motion of the neutral gas (Doppler broadening).[19] The ion energy spread has a width in the CM frame of <0.15 eV except for the previously reported reaction of Sc^+ with C_2H_6, where the width is 0.24 eV. The second effect has a width in the CM frame of $\sim 0.49E^{1/2}$ for the reactions of Sc^+, Y^+, La^+, and Lu^+ with CH_4 and C_2H_6.[19] The resultant energy distribution effectively broadens any sharp features in the excitation function. When model cross sections are compared to experimental data, the calculated cross sections are convoluted with both sources of experimental and energy broadening.[17]

Raw ion intensities are converted to absolute cross sections as described previously.[17] The accuracy of our absolute cross sections is estimated to be ±20%. Uncertainties at low cross-section values are generally about $\pm 10^{-19}$ cm^2, primarily because of random counting noise (typically ≤10 counts/s). Uncertainties are higher for MH^+ channels because of overlap in the mass spectrometer with the intense neighboring M^+ peak. In some cases, this results in scattered data below the energies at which the MH^+ can be produced. In such circumstances, these data points have been removed for clarity.

Ion Sources. In this experiment, ions are produced in a surface ionization (SI) source. Here, MCl_3 (where M = Sc, Y, La, or Lu)[20] is vaporized in a resistively heated oven and directed at a rhenium filament that is resistively heated. A minimum temperature of ≃2000 K (as measured by optical pyrometry) is necessary for these studies, while the maximum temperature attainable is ≃2500 K. It is generally assumed that a Maxwell–Boltzmann distribution accurately describes the populations of the electronic states of the ions. Evidence supporting this assumption has been discussed previously.[7] Table I gives these populations for the ions at 2200 K. Since all transitions between states in Table I are parity forbidden, the radiative lifetimes of the excited states (on the order of seconds long)[21] are expected to be much greater than the flight time between the ionization and reaction regions (~10–100 μs). Thus, very few excited ions radiatively relax before reaction.

In previous studies, reactant ion state populations were varied by using the more vigorous ionization method of electron impact (EI) and, in some cases, by relaxing the EI beam to pure ground-state ions in a high-pressure drift cell. Neither of these methods is used in this study since we have found no suitably volatile yet thermally stable compounds of scandium, yttrium, lanthanum, or lutetium that produce atomic transition-metal ions without impurities of the same mass during EI ionization.

(11) Sunderlin, L.; Aristov, N.; Armentrout, P. B. *J. Am. Chem. Soc.* **1987**, *109*, 78–89.
(12) Tolbert, M. A.; Beauchamp, J. L. *J. Am. Chem. Soc.* **1984**, *106*, 8117–8122.
(13) Huang, Y.; Wise, M. B.; Jacobson, D. B.; Freiser, B. S. *Organometallics* **1987**, *6*, 346–354.
(14) Schilling, J. B.; Beauchamp, J. L. *J. Am. Chem. Soc.* **1988**, *110*, 15–24.
(15) Watson, P. L. *J. Am. Chem. Soc.* **1983**, *105*, 6491–6493.
(16) Bunel, E.; Burger, B. J.; Bercaw, J. E. *J. Am. Chem. Soc.* **1988**, *110*, 976–978. Thompson, M. E.; Baxter, S. M.; Bulls, A. R.; Burger, B. J.; Nolan, M. C.; Santarsiero, B. D.; Schaefer, W. P.; Bercaw, J. E. *J. Am. Chem. Soc.* **1987**, *109*, 203–219.
(17) Ervin, K. M.; Armentrout, P. B. *J. Chem. Phys.* **1985**, *83*, 166–189.
(18) Ervin, K. M.; Armentrout, P. B. *J. Chem. Phys.* **1986**, *84*, 6738–6749, 6750–6760. Burley, J. D.; Ervin, K. M.; Armentrout, P. B. *Int. J. Mass Spectrom. Ion Processes* **1987**, *80*, 153–175.
(19) Chantry, P. J. *J. Chem. Phys.* **1971**, *55*, 2746–2759.
(20) The metal chlorides are obtained from Aesar and are used without further purification.
(21) Garstang, R. H. *Mon. Not. R. Astron. Soc.* **1962**, *124*, 321; private communication.

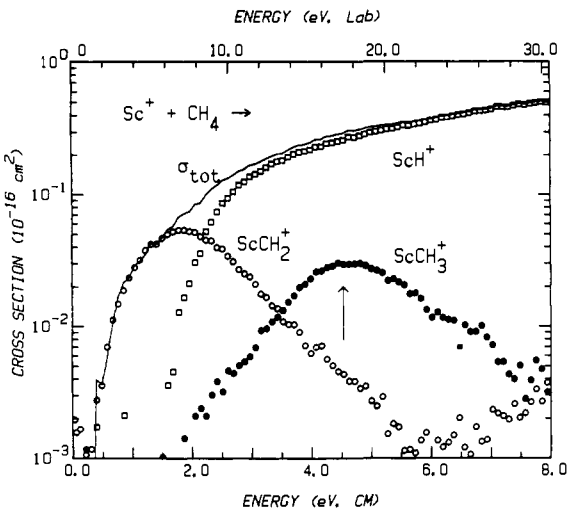

Figure 1. Variation of product cross sections with translational energy in the laboratory frame (upper axis) and center-of-mass frame (lower axis) for the reaction of Sc^+ with CH_4. The arrow indicates $D°(H–CH_3)$ at 4.54 eV.

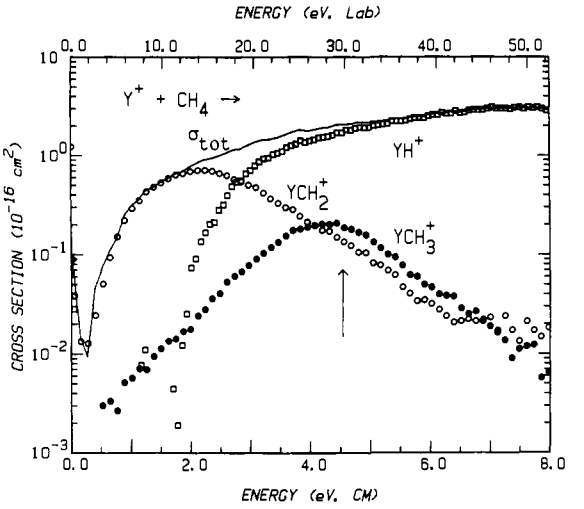

Figure 2. Variation of product cross sections with translational energy in the laboratory frame (upper axis) and center-of-mass frame (lower axis) for the reaction of Y^+ with CH_4. The arrow indicates $D°(H–CH_3)$ at 4.54 eV.

Results

Methane. Cross sections for the products of the reaction of Sc^+, Y^+, La^+, and Lu^+ with methane are shown in Figures 1–4. In all cases, the three products observed are given by reactions 1–3.

$$M^+ + CH_4 \rightarrow MH^+ + CH_3 \quad (1)$$

$$M^+ + CH_4 \rightarrow MCH_2^+ + H_2 \quad (2)$$

$$M^+ + CH_4 \rightarrow MCH_3^+ + H \quad (3)$$

The results for the group 3 ions are quite similar to those seen in the reactions of other early-transition-metal ions, Ti^+,[7] V^+,[8] and Cr^+,[9] with methane, although MCH^+ is also observed for Ti^+ and V^+. At low energy, the dominant process is reaction 2. At higher energy, the cross section for reaction 2 falls off as the cross sections for reactions 1 and 3 rise, with reaction 1 predominating. Lu^+ differs somewhat from the other ions in that the apparent threshold for reaction 2 is nearly the same as that for reaction 1. The smooth appearance of the total cross sections suggests that reactions 1 and 2 are closely coupled. Indeed, the MCH_2^+ products cannot decompose until 4.8 eV. Thus, the decline in this product must be a result of competition with reactions 1 and 3.

The cross sections for MCH_3^+ are seen to peak at 4–5 eV. Above 5 eV, the cross sections for MCH_3^+ fall off as $E^{-0.3}$, $E^{-0.4}$,

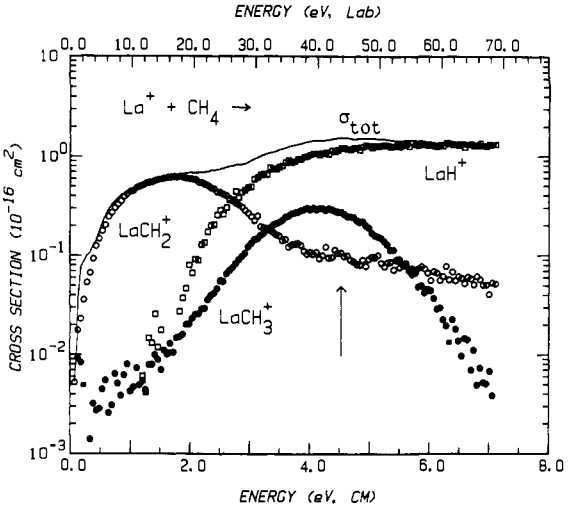

Figure 3. Variation of product cross sections with translational energy in the laboratory frame (upper axis) and center-of-mass frame (lower axis) for the reaction of La^+ with CH_4. The arrow indicates $D°(H–CH_3)$ at 4.54 eV.

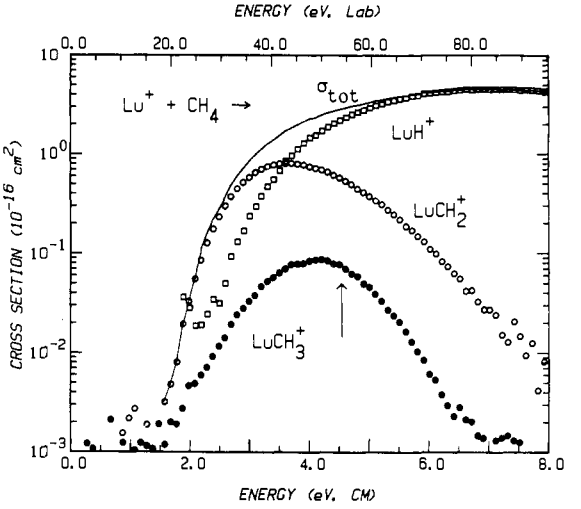

Figure 4. Variation of product cross sections with translational energy in the laboratory frame (upper axis) and center-of-mass frame (lower axis) for the reaction of Lu^+ with CH_4. The arrow indicates $D°(H–CH_3)$ at 4.54 eV.

$E^{-0.7}$, and $E^{-0.9}$ for M = Sc, Y, La, and Lu, respectively. The falloff in the cross sections for MCH_3^+ can be explained by decomposition, reactions 4–6. The dominant process, reaction 4,

$$M^+ + CH_4 \rightarrow MCH_3^+ + H \rightarrow M^+ + CH_3 + H \quad (4)$$

$$M^+ + CH_4 \rightarrow MCH_3^+ + H \rightarrow MCH_2^+ + 2H \quad (5)$$

$$M^+ + CH_4 \rightarrow MCH_3^+ + H \rightarrow MCH^+ + H_2 + H \quad (6)$$

has a threshold of 4.54 eV that is consistent with the apparent onset of decomposition in all cases. MCH^+ is not seen for any of the metals studied, ruling out reaction 6. Reaction 5 is a minor decomposition route, as indicated by the slight rise in the cross section for $ScCH_2^+$ at 6 eV and the breaks in the cross sections for YCH_2^+ and $LaCH_2^+$ at 5–6 eV. No similar effect is seen in the cross section for $LuCH_2^+$. Given the small cross section of the $LuCH_3^+$ product, it is not surprising that no effect is seen in the cross section for $LuCH_2^+$. The threshold for reaction 5 is 4.52 eV above the threshold for formation of MCH_2^+, higher than the threshold for reaction 4.

The cross sections for MH^+ are not seen to fall off but instead remain approximately flat (M = Y, La, and Lu) or continue to rise (M = Sc). Like MCH_3^+, the MH^+ product can decompose beginning at 4.54 eV. The lack of decomposition for MH^+ has been explained for reactions of other metal ions[7–10] by noting that

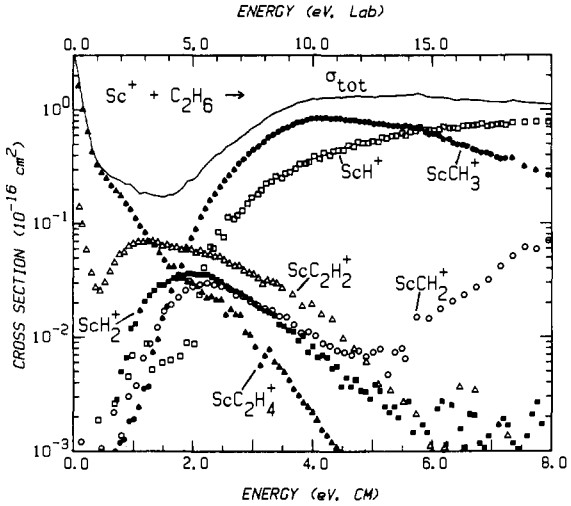

Figure 5. Variation of product cross sections with translational energy in the laboratory frame (upper axis) and center-of-mass frame (lower axis) for the reaction of Sc^+ with C_2H_6.

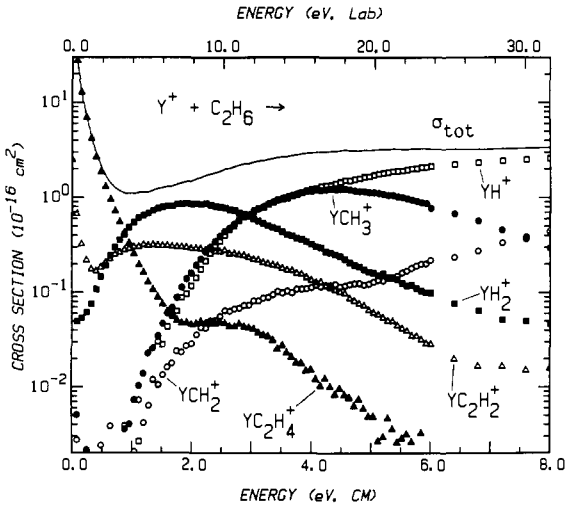

Figure 6. Variation of product cross sections with translational energy in the laboratory frame (upper axis) and center-of-mass frame (lower axis) for the reaction of Y^+ with C_2H_6.

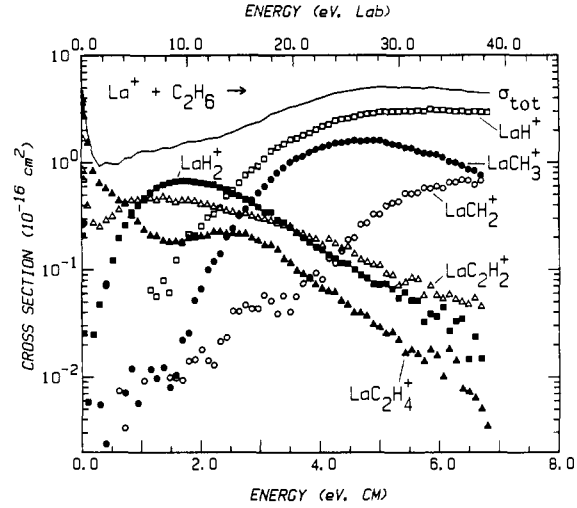

Figure 7. Variation of product cross sections with translational energy in the laboratory frame (upper axis) and center-of-mass frame (lower axis) for the reaction of La^+ with C_2H_6.

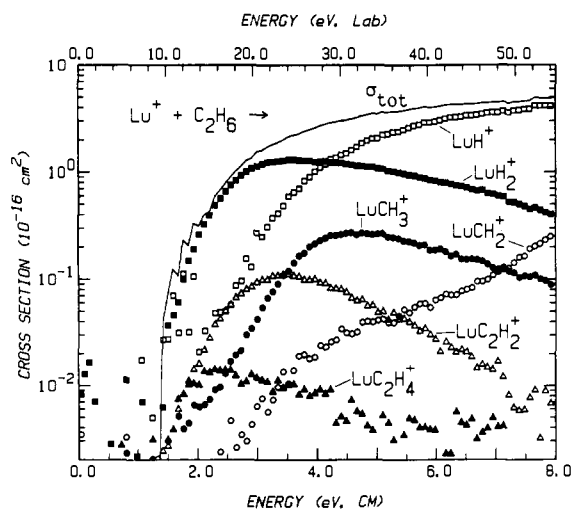

Figure 8. Variation of product cross sections with translational energy in the laboratory frame (upper axis) and center-of-mass frame (lower axis) for the reaction of Lu^+ with C_2H_6.

the neutral product in reaction 1, CH_3, can carry away more energy than the neutral product in reaction 3, H. This leaves MCH_3^+ with more internal energy than MH^+ such that the former ion begins to decompose at its thermodynamic limit, while the latter ion does not.

Ethane. Figures 5–8 show the excitation functions for the various product channels in the reaction of ethane with Sc^+, Y^+, La^+, and Lu^+, respectively. The data for the reaction of Sc^+ with C_2H_6 has been published previously[11] and is provided here for comparison. The products seen are given by reactions 7–12. In

$$M^+ + C_2H_6 \rightarrow MH^+ + C_2H_5 \quad (7)$$

$$M^+ + C_2H_6 \rightarrow MH_2^+ + C_2H_4 \quad (8)$$

$$M^+ + C_2H_6 \rightarrow MCH_2^+ + CH_4 \quad (9)$$

$$M^+ + C_2H_6 \rightarrow MCH_3^+ + CH_3 \quad (10)$$

$$M^+ + C_2H_6 \rightarrow MC_2H_2^+ + 2H_2 \quad (11)$$

$$M^+ + C_2H_6 \rightarrow MC_2H_4^+ + H_2 \quad (12)$$

most respects the data for the different metals are quite similar, although Lu^+ has distinct low-energy behavior. Like Sc^+, Y^+ and La^+ are seen to singly and doubly dehydrogenate ethane (reactions 11 and 12) in exothermic reactions, as shown by the fact that the cross sections rise with decreasing energy as low as we can measure. At higher energies, the $MC_2H_2^+$ products exhibit an apparently endothermic feature, as does the $MC_2H_4^+$ product for Y and La. Lu^+ shows only a single endothermic feature for both reactions 11 and 12. These cross sections fall off at higher energies, and MH_2^+ become the dominant product for Y^+, La^+, and Lu^+. At still higher energies, the MH_2^+ cross section declines, and MH^+ and MCH_3^+ are the main products. Some MCH_2^+ is also seen.

As with methane, most of the cross sections fall off at high energy due to dissociation of energetic products. The cross sections for MCH_3^+ fall off at or slightly higher than 3.89 eV, the threshold for reaction 13. As with methane, the MCH_3^+ product decom-

$$M^+ + C_2H_6 \rightarrow MCH_3^+ + CH_3 \rightarrow M^+ + 2CH_3 \quad (13)$$

poses primarily to M^+ but also into MCH_2^+ as evidenced by the rise in the MCH_2^+ cross section above ~5 eV. Again, the MH^+ cross sections do not fall off over the energy range covered for a comparable reason to that discussed above for the methane system.

Temperature Dependence. When the filament temperature of the SI source is varied, varying amounts of excited-state ions can be formed. Where possible, filament temperature dependence studies were done in order to determine the contributions of excited states to the observed cross section. This analysis assumes that a Maxwell–Boltzmann distribution at the filament temperature is correct and recognizes uncertainties in the cross sections of ±20%. The technique is too insensitive to detect relatively small

Table II. Fitting Parameters for Methane[a]

product	n	E_0
ScH^+	1.2 ± 0.1	2.02 ± 0.06
$ScCH_2^+$	1.9 ± 0.9	0.51 ± 0.23
$ScCH_3^+$	2.0 ± 0.2	≡1.98
YH^+	1.4 ± 0.2	2.24 ± 0.15
YCH_2^+	1.5 ± 0.1	0.65 ± 0.13
YCH_3^+	1.9 ± 0.3	≡1.96
LaH^+	1.0 ± 0.5	2.14 ± 0.23
$LaCH_2^+$	1.4 ± 0.2	0.52 ± 0.06
$LaCH_3^+$	1.5 ± 0.2	≡2.15
LuH^+[b]	1.8 ± 0.7	2.87 ± 0.33
$LuCH_2^+$[b]	1.2 ± 0.2	2.29 ± 0.05
$LuCH_3^+$[b]	0.9 ± 0.2	≡2.58

[a] Unless otherwise noted, these fits use eq 15 and include all states with equal reactivity and populations according to Table I. ≡ means parameter held to this value. [b] These fits use eq 14.

differences in the reactivity of particular states.

No filament temperature dependence was seen over a range of at least 2000–2500 K for reactions 2 and 7–12 with M = Sc. Over this range, the ^1D state population changes from 5.1% to 7.0%, a relative change of ≃40%. The populations of more highly excited states change even more. As this change is somewhat greater than our cross-section error limits, the lack of an observable change in the cross section indicates that most of the reactivity seen is due to the ground state. This result is in contrast with other early transition metals, where low-spin states have been found to be far more reactive than high-spin states for M = Ti,[7] V,[8] and Cr.[9] No filament temperature dependence was seen from 2000–2500 K for reactions 1–3 and 7–12 for M = Y, from 1850–2450 K for reactions 1 and 2 for M = La, or from 1950–2300 K for reaction 1–3 for M = Lu. This rules out dominance of these reactions by states above the a^1D in the case of Y^+, above the a^3D in the case of La^+, and above the ground state for Lu^+. Conclusive temperature dependence data were not obtained on the other reactions, but on the basis of the results for the other reactions, there is no reason to believe that any temperature dependence would be observed.

Thermochemical Analysis

Theory[22] and experiment[5,11,23,24] indicate that endothermic reaction cross sections can be parametrized in the threshold region by function 14, where σ_0 is a scaling factor, E is the relative

$$\sigma(E) = \sigma_0(E - E_0)^n/E^m \qquad (14)$$

translational energy of the reactants, n and m are adjustable parameters, and E_0 is the reaction endothermicity. As in previous studies,[8,25] we have utilized $m = 1$. This form is expected to be the most appropriate for translationally driven reactions[26] and has been found to work exceptionally well in a number of previous studies of both atom–diatom reactions and polyatomic reactions.[4-11,23,27] The other parameters (σ_0, n, and E_0) are optimized by using a nonlinear least-squares analysis to give the best fit to the data after convoluting over the experimental energy distribution. Error limits for E_0 are calculated from the range in the threshold values for different data sets and the error in the absolute energy scale.

(22) See discussion in ref 23.
(23) Aristov, N.; Armentrout, P. B. *J. Am. Chem. Soc.* **1986**, *108*, 1806–1819.
(24) Armentrout, P. B.; Beauchamp, J. L. *J. Chem. Phys.* **1981**, *74*, 2819–2826. Armentrout, P. B.; Beauchamp, J. L. *J. Am. Chem. Soc.* **1981**, *103*, 784–791.
(25) Aristov, N.; Armentrout, P. B. *J. Phys. Chem.* **1986**, *90*, 5135–5140.
(26) Chesnavich, W. J.; Bowers, M. T. *J. Phys. Chem.* **1979**, *83*, 900–905.
(27) Boo, B. H.; Armentrout, P. B. *J. Am. Chem. Soc.* **1987**, *109*, 3549–3559. Ervin, K. M.; Armentrout, P. B. *J. Chem. Phys.* **1987**, *86*, 2659–2673. Elkind, J. L.; Armentrout, P. B. *J. Phys. Chem.* **1984**, *88*, 5454–5456. Armentrout, P. B. In Structure/Reactivity and Thermochemistry of Ions; Ausloos, P., Lias, S. G., Eds.; Reidel: Dordrecht, The Netherlands, pp 1987; pp 97–164.

Table III. Fitting Parameters for Ethane[a]

product	n	E_0
YH^+	1.5 ± 0.3	1.98 ± 0.21
YH_2^+	1.9 ± 0.1	0.41 ± 0.07
YCH_2^+	1.9 ± 0.6	1.19 ± 0.12
YCH_3^+	2.7 ± 0.2	1.30 ± 0.05
LaH_2^+	1.3 ± 0.3	0.65 ± 0.08
$LaCH_2^+$	2.8 ± 1.4	1.31 ± 0.60
$LaCH_3^+$	3.5 ± 0.4	1.50 ± 0.15
LuH^+[b]	1.9 ± 0.5	2.57 ± 0.35
LuH_2^+[b]	1.7 ± 0.4	1.67 ± 0.19
$LuCH_2^+$[b]	1.8 ± 0.1	2.41 ± 0.33
$LuCH_3^+$[b]	3.2 ± 0.4	1.92 ± 0.21
$LuC_2H_2^+$[b]	1.4 ± 0.2	1.83 ± 0.08
$LuC_2H_4^+$[b]	2.0 ± 0.6	1.04 ± 0.48

[a] Unless otherwise noted, these fits use eq 15 and include all states with equal reactivity and populations according to Table I. [b] These fits use eq 14.

Table IV. Heats of Formation Used in Deriving Experimental Results[a]

neutral	$\Delta H°_{298}$, eV	neutral	$\Delta H°_{298}$, eV
H	2.26 (0.00)	C_2H_2	2.35 (0.01)
CH_2	4.00 (0.04)	C_2H_4	0.54 (0.01)
CH_3	1.51 (0.01)	C_2H_5	1.23 (0.02)[b]
CH_4	−0.78 (0.01)	C_2H_6	−0.87 (0.01)[c]

[a] All values except where noted are from: Chase, M. W., Jr.; et. al. *J. Phys. Chem. Ref. Data* **1985**, *14*, suppl. 1 (JANAF Tables). Uncertainties are in parentheses. [b] Brouard, M.; Lightfoot, P. D.; Pilling, M. J. *J. Phys. Chem.* **1986**, *90*, 445–450. [c] Pedley, J. B.; Naylor, R. D.; Kirby, S. P. *Thermochemical Data of Organic Compounds*, 2nd ed.; Chapman and Hall: London, 1986.

Table V. Experimental Bond Energies of Group 3 Ions to Hydrocarbons (eV)[a] at 298 K

ligand	Sc^+	Y^+	La^+	Lu^+
H	2.48 ± 0.09[b]	2.70 ± 0.06[b]	2.52 ± 0.09[b]	2.11 ± 0.16[b]
2H	5.01 ± 0.13[c]	5.52 ± 0.07	5.28 ± 0.08	4.26 ± 0.19
HM^+–H	2.53 ± 0.16	2.82 ± 0.09	2.76 ± 0.12	2.15 ± 0.25
CH_2	4.27 ± 0.23	4.13 ± 0.13	4.26 ± 0.06	≥2.49 ± 0.05
CH_3	2.56 ± 0.13[c]	2.58 ± 0.05	2.39 ± 0.15	1.97 ± 0.21
C_2H_2	3.38 ± 0.10[c]	≥3.07	≥2.82	≥1.39 ± 0.08
C_2H_4	≥1.52 ± 0.05[c]	≥1.26	≥1.01	

[a] Multiply by 23.06 to derive values in kilocalories per mole. [b] Values from ref 6. The 298 K values given here are higher than the 0 K values reported in ref 6 by $3kT/2$, 0.04 eV. [c] Values from ref 11.

A complication in this study is that the data generally involve the reactivity of a distribution of electronic states. This is handled by an explicit sum over the contributions of individual states, denoted by i, weighted by their populations, g_i, as shown in eq 15. Here, E_0 is the threshold for reaction of the lowest J state

$$\sigma(E) = \sum_i g_i\sigma_{i0}(E - E_0 + E_i)^n/E^m \qquad (15)$$

of the ion, and E_i is the electronic excitation of each particular J state (for Sc^+ and Y^+, where the splitting of J levels within an electronic state is small, the J averaged values given in Table I are used). For Sc^+, Y^+, and La^+, it is assumed that n, m, and σ_{i0} in eq 15 are the same for all states. In the absence of evidence to the contrary, this is our standard procedure for cases such as these[4] and is roughly consistent with the expected reactivity of the various states, discussed below. In the case of Lu^+, it is assumed that the only state that reacts is the ground state, since the first excited state is not significantly populated and is expected to react inefficiently, as discussed below. In contrast to the other systems, fits to the Lu^+ data using eq 14 are better visually according to statistical tests than fits using eq 15. Threshold values are determined by comparison to several data sets, usually over a range of SI filament temperatures. The lack of filament temperature dependence seen for the measured thresholds or observed cross sections suggests that the assumption of equal reactivity is not greatly in error. Tables II and III summarize the results of

these analyses for the methane and ethane systems, respectively.

The threshold energies for a reaction like process 16 are converted to thermochemical values of interest using eq 17. The

$$M^+ + BC \rightarrow MB^+ + C \quad (16)$$

$$D°(M^+–B) = \Delta H_f°(B) + \Delta H_f°(C) - \Delta H_f°(BC) - E_0 \quad (17)$$

auxiliary thermochemical data required here are listed in Table IV. Thermochemical values derived from the thresholds in Tables II and III are listed in Table V. Expression 17 assumes that the neutral reactants and the products formed at the threshold of an endothermic reaction are characterized by a temperature of 298 K in all degrees of freedom. Equation 17 also implicitly assumes that there are no activation barriers in excess of the endothermicity. This assumption is generally true for ion–molecule reactions and has been explicitly tested a number of times.[27] Furthermore, theoretical calculations on the related reaction of Sc^+ with H_2 found that this reaction can proceed without barriers in excess of the endothermicity.[28]

MH^+. Bond energies for MH^+, Table V, have been previously derived from analysis of reaction 18. We expect these values to

$$M^+ + H_2 \rightarrow MH^+ + H \quad (18)$$

be more accurate than those derived from the methane and ethane systems for several reasons. H_2 is the simplest system in which this bond can be measured. This minimizes effects due to competing channels and internal energy of reactants and products. The H_2 system has been more extensively studied, and the means of analyzing the data are well established.[5] Finally, the experiment can also be done with D_2. This reduces the experimental problem of resolving the MH^+ peak from the comparatively large M^+ peak. Thus, the data in this paper are primarily a check of the previous data.

Reaction 1 gives bond energies of $D°(Sc^+–H) = 2.52 \pm 0.06$ eV, $D°(Y^+–H) = 2.30 \pm 0.15$ eV, $D°(La^+–H) = 2.40 \pm 0.23$ eV, and $D°(Lu^+–H) = 1.67 \pm 0.33$ eV. Reaction 7 gives $D°(Sc^+–H) = 2.57 \pm 0.15$ eV,[11] $D°(Y^+–H) = 2.38 \pm 0.21$ eV, and $D°(Lu^+–H) = 1.80 \pm 0.35$ eV. The threshold for reaction 7 for M = La was unobtainable due to mass overlap with La^+ and LaH_2^+. The values for Sc^+ and La^+ are in good agreement with the H_2 thermochemistry, and the Lu^+ values are within the large experimental errors, but the Y^+ bond strengths derived from reactions 1 and 7 are significantly low. It is unlikely that there are barriers to reactions 1 and 7 for Y^+, but not for the other ions, particularly since the isolobal reaction 18 has no barriers. Apparently, either there is a kinetic shift in the thresholds caused by competition with other channels or the cross sections are inappropriately modeled by our theoretical cross-section form. A kinetic shift of this type was seen in the reaction of Fe^+ with C_3H_8 to form FeH^+.[10] On the other hand, the data may indicate that $D°(Y^+–H)$ derived from the H_2 system is somewhat high. The bond strength is noticeably higher than that for the neighboring ions Sc^+ and La^+. However, until there is better evidence suggesting that the value $D°(Y^+–H) = 2.70 \pm 0.06$ eV is incorrect, we believe that it is more reliable and more consistent with the other $M^+–H$ thermochemistry.

MH_2^+. Analysis of reaction 8 gives the values in Table V. Note that the two-ligand bond energies exceed the H–H bond energy, 4.52 eV, except in the case of Lu^+. Thus, ScH_2^+, YH_2^+, and LaH_2^+ are stable with respect to dissociation, while LuH_2^+ is unstable by 0.26 ± 0.19 eV. The fact that LuH_2^+ is seen indicates that there is a barrier to dissociation and thus that there is a barrier in excess of the endothermicity to insertion of Lu^+ into H_2. This is consistent with the dynamics observed for reaction of Lu^+ with H_2.[6]

MCH_2^+. The values listed in Table V for $D°(M^+–CH_2)$ are taken exclusively from the methane data. The only previous value for comparison comes from work of Hettich and Freiser on La^+.[29] They found from both reactivity and photodissociation studies that $D°(La^+–CH_2) = 4.6 \pm 0.2$ eV, in reasonable agreement with the value determined here.

Fits to the ethane data (reaction 9) lead to values that are lower by 0.85 ± 0.25, 1.22 ± 0.18, 1.47 ± 0.60, and 0.80 ± 0.33 eV for Sc^+, Y^+, La^+, and Lu^+, respectively. This suggests that there are barriers for reaction 9, consistent with earlier work that also found barriers to formation of MCH_2^+ in reactions of Sc^+[11] and V^+[8] with hydrocarbons larger than methane. This observation has been previously discussed for Sc^+.[11] Theoretical studies[30] suggest that reaction 9 can have substantial barriers, while reaction 2 can have little or no barrier. For example, methane elimination from $HPdCH_3$ is calculated to have a barrier of 0.45 eV, while H_2 elimination from HPdH has a barrier of only 0.07 eV. Since ion-induced dipole attraction is sufficient to overcome barriers this small, the thermochemistry for MCH_2^+ derived from the methane system should be unaffected by barriers. However, there may be a barrier to reaction 2 for M = Lu, as discussed below. This means that the derived bond energy should be taken as a lower limit, $D°(Lu^+–CH_2) \geq 2.49 \pm 0.05$ eV.

Given the MCH_2^+ thermochemistry in Table V, $\simeq$1% of the Y^+ ions (the a^3F and higher states) and $\simeq$2% of the La^+ ions (the a^3P and higher states) should react exothermically. A small exothermic cross section is seen at low energy for M = Y, Figure 2, but no exothermic cross section is seen for M = La, Figure 3. Either excited-state La^+ ions do not react very efficiently or there is a barrier to production of ground-state products for these ions.

A preliminary analysis of the Sc^+ data for reaction 2 found a threshold of 0.42 ± 0.11 eV using single-state fits.[11] This was used to give a lower limit to the bond energy of 4.05 ± 0.11 eV because it was unclear whether the triplet ground state or the singlet first excited state dominated the reactivity seen. Further temperature dependence studies discussed above indicate that the reactivity can be assumed to be due primarily to the ground state.

MCH_3^+. The threshold of reaction 3 is very difficult to interpret for the metal ions studied here because of the small cross section, strong competition by the other two channels, and the slow rise of the cross section, as seen in Figures 1–4. This has been noted before for Ti^+[7] and V^+.[8] Reaction 10 is more useful because of its larger cross section, relative lack of competition, and steeper rise from threshold. Thus, the bond energies for MCH_3^+ listed in Table V are taken from the ethane system. For Sc^+, the value listed includes results from the analysis of reaction 19.[11]

$$Sc^+ + C_3H_8 \rightarrow ScCH_3^+ + C_2H_5 \quad (19)$$

The derived bond strengths give expected thresholds for reaction 3 for M = Sc, Y, La, and Lu of 1.98, 1.96, 2.15, and 2.58 eV, respectively. If E_0 is held to these values with $m = 1$, the data can be reproduced nicely for M = Sc and Lu when $n = 2.0 \pm 0.2$ and 0.9 ± 0.2, respectively. For M = Y and La, the best fits to the data use $n = 1.9 \pm 0.3$ and 1.5 ± 0.2, respectively; however, the data are larger than the fit at energies below the threshold for the ground state. This deviation is evident in that the apparent thresholds for the MCH_3^+ cross sections in Figures 2 and 3 are well below the expected thresholds. These deviations may be due to the efficient reactions of small amounts of excited states. Similar effects are not observed in any other product channel in either the methane or ethane systems.

$MC_2H_2^+$ and $MC_2H_4^+$. The thermochemistries of $ScC_2H_2^+$ and $ScC_2H_4^+$ have been previously reported,[11] Table V. The exothermicity of reactions 11 and 12 gives lower bounds on the bond strength of Y^+ and La^+ to C_2H_4 and C_2H_2. $D°(Y^+–C_2H_4)$ and $D°(La^+–C_2H_4)$ were concluded to be $\geq$1.41 eV on the basis of this observation.[13] A significant question for both metals is whether the reaction is exothermic for the ground state or for some excited state. Such information can be determined by examining the filament temperature dependence of the cross section or by comparing the cross section to the close-collision (Langevin)[31] cross

(28) Rappe, A. K.; Upton, T. H. *J. Chem. Phys.* **1986**, *85*, 44400–4410.
(29) Hettich, R. L.; Freiser, B. S. *J. Am. Chem. Soc.* **1987**, *109*, 3543–3548.
(30) Steigerwald, M. L.; Goddard, W. A., III *J. Am. Chem. Soc.* **1984**, *106*, 308–311. Low, J. J.; Goddard, W. A., III *J. Am. Chem. Soc.* **1984**, *106*, 8321–8322.

section, σ_L, given by eq 20, where α is the polarizability of the

$$\sigma_L\ (\text{Å}^2) = 16.9(\alpha/E)^{1/2} \qquad (20)$$

neutral in cubic angstroms and E is the energy in electronvolts. This gives $\sigma_L = 27.0E^{-1/2}$ for CH_4 and $35.3E^{-1/2}$ for C_2H_6.[32]

The cross section for reaction 15 for M = Y is 20% of σ_L at 0.1 eV, indicating that ≥20% of the ions react at this energy (since they could react with less than unit efficiency). Since the population of states higher than the a^3D is less than 9%, one of the two lowest states must be responsible for the reactivity seen. Given the large population in the ^3D state, we can conclude only that the reaction is exothermic for that state. This gives $D°(Y^+–C_2H_4) \geq 1.26$ eV. Since no filament temperature dependence was seen in the low-energy cross section for reaction 11, we conclude here as well that reaction 11 must be exothermic for the ^3D state, giving $D°(Y^+–C_2H_2) \geq 3.07$ eV.

Reactions 11 and 12 are also exothermic for La^+. The highest J level of the a^3D state has an excitation energy of 0.403 eV and a population of 5.5%; higher excited states have a population of less than 2%. The cross sections for reactions 11 and 12 at 0.1 eV are 0.35% and 1.3% of σ_L, respectively. Given the lack of state specificity seen for the group 3 ions and the relatively large size of the experimental cross sections, it is reasonable to assign the exothermic reactivity seen to the a^3D and lower states. This gives $D°(La^+–C_2H_4) \geq 1.01$ eV and $D°(La^+–C_2H_2) \geq 2.82$ eV.

Unlike the other group 3 ions, Lu^+ does not exothermically dehydrogenate ethane. Thus, the threshold for single and double dehydrogenation can be measured, Table III. These thresholds indicate bond energies of $D°(Lu^+–C_2H_2) = 1.39 \pm 0.08$ eV and $D°(Lu^+–C_2H_4) = 0.38 \pm 0.48$ eV. As discussed below, it is possible that there is a barrier in excess of the actual endothermicity for both of these reactions. Therefore, the value for $D°(Lu^+–C_2H_2)$ is a lower limit and we do not quote a value on the latter bond energy since we can conclude only that $D°(Lu^+–C_2H_4)$ is positive.

Comparisons to Theory. Theoretical values for $D°(Sc^+–H)$, $D°(Y^+–H)$, and $D°(HSc^+–H)$ have been discussed previously.[6,11] Theoretical calculations by Schilling and Goddard[33] give $D°(Sc^+–CH_3) = 2.34$ eV and $D°(Y^+–CH_3) = 2.50$ eV, while Bauschlicher obtains $D°(Sc^+–CH_3) = 2.42$ eV.[34] As with $M^+–H$ bond energies,[6] the theoretical values are in reasonable agreement with (although somewhat lower than) the experimental values. A theoretical value for $D_e(Sc^+–CH_2)$ of 2.95 eV has also been obtained.[35] This is poorer agreement although the geometry was not optimized, all electrons were not correlated, and the level of calculation was somewhat lower than the other calculations. Previous theoretical calculations on metal methylidenes have also given lower bond energies than experiment.[36]

Periodic Trends. It has been pointed out for Sc^+,[11] Ti^+,[7] V^+,[37] Nb^+, Rh^+, and La^+[38] that M–H and M–C single-, double-, and triple-bond strengths correlate well with hydrocarbon single-, double-, and triple-bond strengths. Since MCH^+ is not seen in reaction with methane and ethane for the group 3 ions, triple-bond strengths cannot be measured. Indeed, since the group 3 ions have only two valence electrons, a full triple bond cannot be formed, suggesting that the bonds to CH should be relatively weak.[11,35] This is presumably why no MCH^+ is seen. $M^+–H$, $M^+–CH_3$, and $M^+–CH_2$ bond energies are in the ratios 1:1.03:1.72 for M = Sc, 1:0.96:1.53 for M = Y, 1:0.95:1.69 for M = La, and 1:0.93:≥1.18 for M = Lu. The bond energies $D°(H–H)$, $D°(H–CH_3)$, and $D°(H_2C{=}CH_2)$ are in the ratio 1:1.01:1.65. The correlation thus holds for Sc^+, Y^+, and La^+ but may not hold for Lu^+.

As discussed previously,[3,39] the bond energies of the first- and second-row transition-metal ion hydrides have been found to be equal to an intrinsic bond strength (2.5 eV for the first row and 2.6 eV for the second row) minus some fraction of the energy necessary to promote the ion into a state suitable for bonding. Using the previously published[3] correlations between $D°(M^+–H)$ and E_p leads to estimates of 2.3, 2.4, 2.4, and 1.9 eV for the $M^+–H$ bond energies where M = Sc, Y, La, and Lu, respectively. This is reasonably accurate for the group 3 metal hydride ions.[6]

In all cases, the second metal–hydride bond energy is slightly larger than the first. For Sc^+, Y^+, and La^+, this fits the intrinsic bond energy model,[3,6] since after one bond is formed, the promotion energy for making a second bond is zero. The model predicts that the $HLu^+–H$ bond should be significantly stronger, ~0.7 eV, than the $Lu^+–H$ bond. This may be true, given the error bars of the measurements.

Table V shows that the metal–methyl bond strengths are lower than the hydride bond strengths by -0.08 ± 0.16, $+0.12 \pm 0.08$, $+0.13 \pm 0.18$, and $+0.14 \pm 0.26$ eV, respectively, for M = Sc, Y, La, and Lu. The data suggest that the metal–methyl and metal–hydride bond energies are approximately equal for these species. As discussed previously,[3] $D°(M^+–CH_3)$ is found to be 0.09 ± 0.13 eV stronger than $D°(M^+–H)$ for the early first-row transition metals ($Sc^+–Mn^+$). While more data are needed to determine precisely the trend for second- and third-row transition elements, the group 3 metals are consistent with the conclusion reached for the first-row metals.

$D°(M^+–CH_2)$ should be significantly stronger than $D°(M^+–H)$ or $D°(M^+–CH_3)$ because of the double bond that can form between these divalent ions and CH_2. It has been suggested that the intrinsic strength of a $M^+–C$ π bond is $\simeq 1.6$ eV.[3] The promotion energy necessary for two bonds has been discussed previously.[40] No extra promotion energy is necessary for any of the group 3 ions to form a second bond. Thus, the double-bond strength is predicted to be 4.0, 4.1, 4.1, and 3.5 eV for Sc^+, Y^+, La^+, and Lu^+, respectively. As can be seen in Table V, the predicted values are somewhat low for Sc^+, Y^+, and La^+, while the Lu^+ value is well off. Except for Lu^+, the agreement is good, especially considering the simplicity of the model and the fact that the data base for making such predictions is quite limited. The results for Sc^+, Y^+, and La^+ help confirm that there are no barriers in excess of the endothermicity to forming MCH_2^+ for these metals, while the low $Lu^+–CH_2$ bond energy suggests that there could be a barrier to this reaction. Alternatively, the s^2 configuration of ground-state Lu^+ could lead to very different bonding in the $LuCH_2^+$ molecule compared to the other MCH_2^+ species. Specifically, this molecule could involve a dative interaction between $Lu^+(^1S)$ and $CH_2(^1A_1)$,[36c] rather than a covalent double bond.

The relationship between the intrinsic bond strength model and the bond ratio model can be seen by noting that the *intrinsic* bond strengths[3] (2.5, 2.6, and 4.1 eV for the first row and 2.56, 2.65, and 4.2 eV for the second row) are in the ratio 1:1.04:1.64 for the first row and 1:1.03:1.64 for the second row, very close to the bond strength ratios given above. Thus, when the promotion energy is low (as is true for most early transition metals), both models fit the data.

Discussion

M^+ + Methane. Reaction Mechanism. Some step in the reactions of M^+ with methane seen must break a C–H bond. This step must either be insertion of M^+ into a C–H bond (oxidative addition) to form $HMCH_3^+$, intermediate I, or C–H bond cleavage

(31) Gioumousis, G.; Stevenson, D. P. *J. Chem. Phys.* **1958**, *29*, 294–299.
(32) Polarizabilities taken from: Rothe, E. W.; Bernstein, R. B. *J. Chem. Phys.* **1959**, *31*, 1619–1627.
(33) Schilling, J. B.; Goddard, W. A., III; Beauchamp, J. L. *J. Am. Chem. Soc.* **1987**, *109*, 5573–5580.
(34) Bauschlicher, C. W., private communication.
(35) Alvarado-Swaisgood, A. E.; Harrison, J. F. *J. Phys. Chem.* **1988**, *92*, 2757–2762.
(36) (a) Alvarado-Swaisgood, A. E.; Allison, J.; Harrison, J. F. *J. Phys. Chem.* **1985**, *89*, 2517–2525. (b) Carter, E. A.; Goddard, W. A., III *J. Phys. Chem.* **1984**, *88*, 1485–1490. (c) Carter, E. A.; Goddard, W. A., III *J. Am. Chem. Soc.* **1986**, *108*, 2180–2191.
(37) Aristov, N.; Armentrout, P. B. *J. Am. Chem. Soc.* **1984**, *106*, 4065–4066.
(38) Hettich, R. L.; Freiser, B. S. *J. Am. Chem. Soc.* **1987**, *109*, 3543–3548.
(39) Schilling, J. B.; Goddard, W. A., III; Beauchamp, J. L. *J. Phys. Chem.* **1987**, *91*, 5616–5623.
(40) Tolbert, M. A.; Beauchamp, J. L. *J. Am. Chem. Soc.* **1986**, *108*, 7509–7517.

via a direct process. The first process is thermodynamically more favorable since the broken C–H bond energy (4.54 eV) is replaced by the energy of an M^+–H bond and an HM^+–CH_3 bond. Assuming that $D°(HM^+–CH_3) \simeq D°(HM^+–H)$, the ground state of intermediate I can be estimated to lie 0.47 eV below, 0.97 eV below, 0.73 eV below, and 0.28 eV above the ground-state reactants for M = Sc, Y, La, and Lu, respectively. The ground state of $HMCH_3^+$ is expected to be a singlet for all four metals, since for the group 3 ions only singlet states can have two covalent bonds. Thus, many electronic states of the group 3 elements (including those having the highest populations for Sc^+, Y^+, and La^+, Table I) must change spin in order to form ground-state I. The lowest triplet state of $HMCH_3^+$ should have one electron promoted from a bonding orbital to a nonbonding orbital, suggesting that the triplet states of $HMCH_3^+$ are higher in energy by about half of the M^+–H bond strength ($\simeq$1.2 eV).

Formation of MCH_2^+, which has a singlet ground state, can occur via formation of singlet $HMCH_3^+$ followed by a concerted four-center elimination of H_2. Theoretical calculations[41] suggest that this reaction can occur with little or no barrier if the metal–ligand bonds are covalent and have substantial d character. These conditions are likely to be true for M = Sc^+, Y^+, and La^+. Lu^+ is probably an exception, as the s^2 state of Lu^+ is much lower in energy than states with d orbital occupation, Table I. Thus, there may be little d character in the H–Lu^+–CH_3 bonds such that there may be a barrier in excess of the endothermicity to formation of $LuCH_2^+$, as mentioned above.

An alternative mechanism for dehydrogenation involves formation of I, followed by α-H transfer to M to form $(H)_2M^+$–CH_2 and then reductive elimination of H_2. This is thermodynamically unreasonable for these divalent metals because they lack the four electrons needed to covalently bond all three ligands. It is possible that the $(H)_2M^+$–CH_2 bond is purely dative, but then this intermediate can only lie lower in energy than the $MCH_2^+ + H_2$ products if $D°[(H)_2M^+–CH_2] \simeq D°(M^+–CH_2)$. Since it seems highly unlikely that the strength of such a dative bond is comparable to that for a covalent double bond, we discount this mechanism. Similar thermochemical arguments indicate that the Ti^+ and V^+ analogues of reaction 2 must also occur via a four-center elimination.[7,8]

Intermediate I can also explain reactions 1 and 3, since these can occur by simple bond cleavages of the M^+–C and M^+–H bonds, respectively. If reactions 1 and 2 do share the common intermediate I, the strong competition between these processes can be explained. Decomposition of I via reaction 1 can be favored at high energies despite being more endothermic than reaction 2 because it involves a loose transition state while reaction 2 proceeds through a tight four-center transition state. While this strongly suggests that MH^+ is formed via I, it does not imply that *all* of the MH^+ seen comes from intermediate I.

If the MCH_2^+ reaction channel is depleted by MH^+ (and possibly MCH_3^+) formation, then the cross sections for these products should be coupled. Modeling this competition has been discussed before in the case of the reaction of Cr^+ with methane.[9] Essentially, we find that the threshold analysis for the MCH_2^+ cross section listed in Table II reproduces the sum of the cross section for reaction 2 added to some fraction of the cross section for reaction 1. This combined analysis can be viewed as a fit to the cross section for insertion products. This fraction of $\sigma(MH^+)$ required is 0.8, 0.7, 1.0, and 0.55 for M = Sc, Y, La, and Lu, respectively (with errors of $\sim$0.1). The fits are quite good to about 6 eV for M = Sc, Y, and Lu, while the M = La fit is poor. Although these numbers should not be taken quantitatively, these fractions give an indication that most of the MH^+ seen is due to an insertive mechanism for M = Sc, Y, and La, while the LuH^+ seen is due to similar amounts of both insertion and direct reaction.

Branching Ratios. Branching ratios for competing reactions such as reactions 21 and 22 have been found to be a sensitive indicator of the reaction mechanism.[4] Similarly, the branching

$$M^+ + HD \rightarrow MH^+ + D \quad (21)$$

$$M^+ + HD \rightarrow MD^+ + H \quad (22)$$

ratio for reactions 1 and 3 also reflects the reaction mechanism.[7-10] The arguments involved for reaction with methane have been summarized.[8] The basic results are the following: (1) If the reactions proceed through a statistically behaved intermediate where all degrees of freedom equilibrate, then the branching ratio, $\sigma(MH^+)/\sigma(MCH_3^+)$, should be given by phase space theory (PST)[42] calculations. Since calculations on MH^+ and MCH_3^+ for M = Sc and Y have been performed, much of the data necessary to do PST calculations are available. However, the vibrational frequencies of the doubly degenerate M–C–H bend in MCH_3^+ are still not well-known. More significantly, it is not known if the rotational degrees of freedom at the transition state are the same as those of the separated products, as is assumed in PST. Given the uncertainty in some of the necessary values, the branching ratio is calculated to be between 4 and 20. This confirms our previous conclusions.[8] (2) If the reaction proceeds via a direct mechanism such that not all degrees of freedom equilibrate, $\sigma(MH^+)/\sigma(MCH_3^+)$ should be greater than 20 and can approach a value of 90 for an impulsive process. For example, the high-spin ground state of V^+ shows a cross-section ratio of 4, and the two low-lying high-spin states of Ti^+ show a ratio of 7. These states are expected to react statistically. The low-spin first excited state of V^+ and second excited state of Ti^+, which are considered to react via a direct mechanism, both show a ratio of $\sim$30.[7,8]

At 4 eV, before the MCH_3^+ cross sections begin to fall off, the ratio of ScH^+ to $ScCH_3^+$ is 9:1, the ratio of YH^+ to YCH_3^+ is 7:1, and the ratio of LaH^+ to $LaCH_3^+$ is 4:1. This indicates that these systems are behaving mainly in a statistical manner. The branching ratios for reaction of Sc^+, Y^+, and La^+ with HD favor MH^+ over MD^+ by 2.0:1, 1.4:1, and 1.2:1, respectively.[6] This also indicates primarily statistical behavior with some direct reaction. The ratios decline with mass for both HD and CH_4, suggesting that the reactions become more statistical further down the column. The ratio of LuH^+ to $LuCH_3^+$ is 20:1 at 4 eV. This indicates that this reaction is more direct. The LuH^+ to LuD^+ ratio of 4:1 at higher energies also indicates that the reaction with HD is direct. Note that these conclusions agree with those derived above from comparisons of the MCH_2^+ and MH^+ cross sections.

The values of n used to fit the cross sections for MCH_3^+ for Sc^+, Y^+, La^+, and Lu^+ are 2.0 ± 0.2, 1.9 ± 0.3, 1.5 ± 0.2, and 0.9 ± 0.2, respectively. For comparison, n = 2.8 was found to model the cross section of the analogous reactions of Ti^+[7] and V^+[8] with methane, while n = 1 was used for Cr^+.[9] Qualitatively, Sc^+, Y^+, and La^+ are more like Ti^+ and V^+, which follow an insertive mechanism, while Lu^+ is more like Cr^+, which reacts directly.

Cross-Section Magnitudes. The overall reactivity of Sc^+ with methane is less than that of Y^+, La^+, and Lu^+ by a factor of 5–10, Figures 1–4. Given that the bond energies of H, CH_2, and CH_3 for the first three ions are approximately the same and the bond strengths for Lu^+ are lower, this cannot be an energy effect. The relative electronic energy levels indicate nothing unique about Sc^+ that would make its reactivity so low. Apparently, there is a bottleneck in the reaction for Sc^+ that is less restrictive for the other ions. This bottleneck may be because most of the metal ions produced by SI are in triplet states, yet the dominant reaction mechanism involves formation of $HMCH_3^+$ in a singlet state. Since the heavier elements have greater spin–orbit coupling, the necessary spin change is probably less efficient for Sc^+ than for the other metals. This qualitatively explains why the reactivity of Sc^+ appears to be somewhat more direct than the reactivity of Y^+ and La^+, as discussed above. Unlike the other metal ions, the total cross sections for Sc^+ continues to rise after the other

(41) Steigerwald, M. L.; Goddard, W. A., III *J. Am. Chem. Soc.* **1984**, *106*, 308–311. Rappe, A. K. *Organometallics* **1987**, *6*, 354–357.

(42) Light, J. C.; Pechukas, P. *J. Chem. Phys.* **1965**, *42*, 3281–3291. Grice, M. E.; Song, K.; Chesnavich, W. J. *J. Phys. Chem.* **1986**, *90*, 3503–3509.

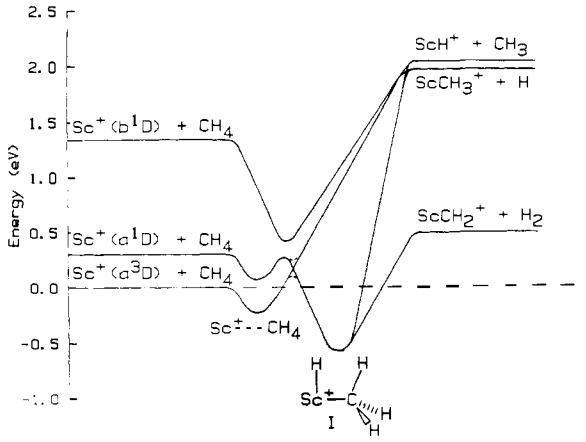

Figure 9. Semiquantitative potential energy surface for the reaction of Sc^+ with CH_4. The solid lines indicate adiabatic surfaces, and the dashed lines indicate an avoided singlet–triplet surface crossing in the entrance channel.

cross sections have leveled off, indicating that direct reaction becomes more efficient at higher translational energies.

Potential Energy Surfaces. In order to further appreciate the reactions of the group 3 metal ions with methane, we need to understand the potential energy surfaces in somewhat more detail. This can be accomplished by using molecular orbital (MO) arguments that have been used previously to explain the reactivity of transition-metal ions with H_2[4] and extended with success to cover the reactions of Ti^+, V^+, Cr^+, and Fe^+ with methane.[7-10] In the case of $Sc^+ + H_2$, these arguments are in accord with detailed ab initio calculations.[28] In correspondence with the H_2 reaction, the primary interaction between the metal ion and methane is the overlap of the methane σ(CH) bonding orbital with the valence s orbital (and to a lesser extent the valence dσ orbital) of M^+. Since there are already two electrons in the σ(CH) orbital to occupy the bonding MO, any electrons in the metal s or dσ orbitals must occupy an antibonding MO, leading to a repulsive interaction. Thus, states with the s orbital occupied are not expected to insert into C–H bonds. If the s and dσ orbitals are empty, then delocalization of the electrons in the σ(CH) orbital onto the metal causes a bonding interaction, which can be strengthened by back-donation from a metal dπ orbital into the empty σ^*(CH) orbital.

These considerations lead to the potential energy surfaces shown for $Sc^+ + CH_4$ in Figure 9. The state that diabatically correlates with the insertion product I is the $b^1D(d^2)$ state, the lowest singlet state that has no s electrons.[43] The attractive surface derived from this state will cross the more repulsive surface derived from the $a^1D(sd)$ first excited state. The surfaces evolving from the a^1D and b^1D states will undergo an avoided crossing, such that the a^1D state *adiabatically* correlates with insertion. The key interaction comes when the repulsive $a^3D(sd)$ state crosses the singlet curve that leads to insertion. To the degree that these surfaces mix, ions in the a^3D state can insert into the C–H bond. This mixing can occur because of spin–orbit coupling. The existence of a reaction bottleneck at this singlet–triplet crossing point has been discussed previously for the reaction of Sc^+ with ethane.[11] $a^3D(sd)$ and $a^1D(sd)$ ions that do not cross onto the insertive surface can react directly to form MH^+ and MCH_3^+, as shown in Figure 9.

Similar surfaces exist for Y^+ and La^+. Specifically, the reactions of the most populous states, $Y^+(^3D)$ and $La^+(^3F)$, must occur via a triplet–singlet surface crossing. As noted above, the relative reactivity of the Sc, Y, and La systems suggests that this crossing is more efficient for the heavier metals. For the case of Lu^+, the $^1D(d^2)$ state lies about 4.5 eV above the ground state.[44]

(43) Actually, the state that diabatically correlates is the $^1G(d^2)$ state since this is the lowest state where both electrons can occupy the *same* d orbital. For simplicity, we show the correlation to the $^1D(d^2)$ state since the low surfaces evolving from these states will avoid one another anyway.

Scheme I

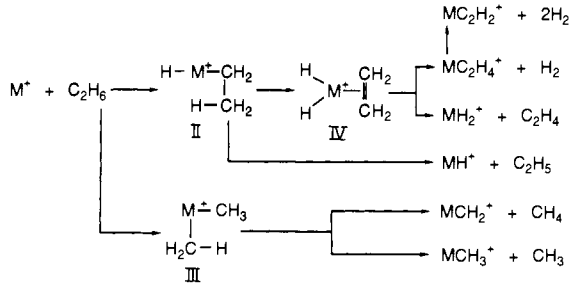

Therefore, it is likely that the potential energy surfaces are significantly different. In particular, the $^1S(s^2)$ state of Lu^+ can be expected to have a fairly repulsive interaction with methane (since the s orbital is doubly occupied), consistent with its more direct reaction mechanism. That Lu^+ reacts at all efficiently may be because the ^1S state does not require a spin change for this insertion.

M^+ + Ethane. Reaction Mechanism. The mechanism for the reaction of M^+ with C_2H_6 has been discussed many times before[11] and is outlined in Scheme I. A more detailed analysis of the individual products that deviate from this basic scheme is given below. Reaction is initiated by insertion into a C–H or C–C bond to form II or III. The lowest energy channels result from a β-hydrogen shift in II to form the dihydrido ethene complex, IV. Reductive elimination of H_2 gives $MC_2H_4^+$, the dominant low-energy product, while ethene loss yields MH_2^+. From $MC_2H_4^+$, a further insertion, β-hydrogen shift, and elimination leads to $MC_2H_2^+$, the second exothermic product. At higher energies, II can decompose by loss of ethyl radical to give MH^+. For initial C–C insertion, on the other hand, the dominant reaction channel is formation of MCH_3^+ by loss of methyl. III can also form MCH_2^+ via reductive elimination of methane in a four-center reaction similar to that discussed above in the methane system. It is also possible that MCH_2^+ is formed after C–H bond insertion, although this was largely ruled out in the case of V^+.[23]

The potential energy surfaces for C–H bond insertion should be similar to those for methane. The most important feature of these surfaces remains the triplet–singlet curve crossings, although the deeper ion-induced dipole well should lower the energy of the crossings. The details of these surfaces have been discussed in detail for the Sc^+ + ethane reaction,[11] although the interaction between the a^1D and b^1D states shown in Figure 9 was neglected in the earlier work.

As with methane, the rections of Y^+, La^+, and Lu^+ with ethane are more efficient than the reactions of Sc^+, with the exception of reactions 11 and 12 for M = Lu, which are endothermic. The large cross sections indicate that low-lying states must be responsible for the majority of the product formation seen, since most of the excited states listed in Table I have insufficient populations even if they react at the collision limit, σ_L. As discussed in ref 11, the inefficiency of the Sc^+ reaction is attributed to the inefficiency of the triplet–singlet surface crossing necessary to insert into the C–H or C–C bond. As with the methane system, the heavier metal ions may react more efficiently because of the enhanced spin–orbit coupling of these metals.

In the case of Lu^+, the failure to observe any exothermic reactions with ethane means there must be barriers along the reaction path, unlike the other three metal ions. Indeed, if $D°(HLu^+–C_2H_5)$ is the same as $D°(HLu^+–H)$, simply inserting into the C–H bond of ethane is 0.10 ± 0.19 eV endothermic. This energy is still well below the threshold for the lowest energy process, dehydrogenation to form $LuC_2H_4^+$ at 1.04 ± 0.48 eV. Since the lowest state that corresponds diabatically to insertion is 4.5 eV high in energy (as discussed for methane), it is feasible that this threshold may correspond to an activation barrier for insertion. If this is correct, other processes that share intermediate

(44) Martin, W. C.; Zalubas, R.; Hagan, L. *Natl. Stand. Ref. Data Ser. (U.S. Natl. Bur. Stand.)* **1978**, *60*.

II, e.g. formation of MH^+ and MH_2^+, are not expected to have barriers higher than this. Since the thresholds for formation of MH^+ and MH_2^+ are higher than 1.5 eV, the thresholds for these processes are believed to corrspond to the thermodynamic values. However, the thermochemistry of $LuC_2H_4^+$ itself cannot be conclusively derived from this reaction because of this possibility. Similarly, the subsequent C–H bond insertion needed to yield $LuC_2H_2^+$ may also have an appreciable barrier such that the threshold for this product is conservatively considered to be an upper limit.

$MC_2H_4^+$. Reaction 12 for M = Sc is unusual in that there are apparently two distinct mechanisms, as deduced from studies of the reaction of Sc^+ with CH_3CD_3.[11] At low energy, 1,2-dehydrogenation predominates, while at high energy, preferential 1,1-dehydrogenation occurs. Mechanistically, this 1,1-dehydrogenation reaction is analogous with the formation of MCH_2^+ in the methane reaction and can occur directly from II. Apparently, the same thing occurs with M = Y and La, as both metals show an exothermic feature and then an abrupt flattening of the cross section at higher energies. Indeed, the reaction of Y^+ with CH_3CD_3 shows that 1,2-dehydrogenation predominates below $\simeq$2 eV, while 1,1-dehydrogenation is favored at higher energies, the region of the $MC_2H_4^+$ plateau in Figure 6. Although definitive results with CH_3CD_3 could not be obtained for La^+ because of mass overlap, we expect that the same competition between 1,2- and 1,1-dehydrogenation occurs.

Only one apparent channel is seen with Lu^+. Again no studies with CH_3CD_3 were performed due to mass resolution restrictions. Since formation of the metal–ethene complex is no longer exothermic, it may not be possible to distinguish the two different channels. It is also possible that one of the channels is not active for M = Lu.

$MC_2H_2^+$. High-Energy Feature. The bimodal energy dependence of the $YC_2H_2^+$ and $LaC_2H_2^+$ products is quite unusual. It has been observed before only with Sc^+[11] and Ti^+.[45] Of the several possible explanations (excited-state reactants, product isomers, excited-state products, and internal energy effects), excited-state reactions and product isomers were ruled out for Sc^+. Instead, we concluded that there are two distinct populations of $ScC_2H_4^+$ that do *not* interconvert: one that reacts completely to form $ScC_2H_2^+$ at low energy and one that reacts only at higher energy to form $ScC_2H_2^+ + H_2$. Similar arguments lead us to the same conclusion for Y^+ and La^+, although detailed filament temperature dependence studies were not performed for La^+. Furthermore, the striking similarity in the $MC_2H_2^+$ channels in Figures 5–7 makes it highly probable that the cause of the two features for Sc^+ is the same for Y^+ and La^+.

The following two explanations, which were previously discused in more detail for Sc^+, are consistent with these two features. One hypothesis involves the probable existence of low-lying triplet and singlet states of $MC_2H_4^+$ and $MC_2H_2^+$. Dehydrogenation of IV would presumably form $MC_2H_4^+$ on a singlet potential energy surface but could also yield a triplet $MC_2H_4^+$ via a curve crossing similar to that in the entrance channel. This would yield two separate populations of $MC_2H_4^+$ which can react further by loss of dihydrogen, one to form ground-state $MC_2H_2^+$ in an exothermic reaction, the other to form an excited state of $MC_2H_2^+$ in an endothermic reaction. This proposal suggests that the reason why little $MC_2H_2^+$ is formed at the lowest energies is that a singlet–triplet curve crossing is necessary for this reaction.

Another explanation for the two $MC_2H_2^+$ features involves energy disposal in the first dehydrogenation. Specifically, it is possible that the exothermic channels in Figures 5–7 correspond to reaction 23a, while the endothermic channels are associated with process 23b, where one of the two molecules of H_2 is left in

$$M^+ + C_2H_6 \rightarrow MC_2H_2^+ + H_2(v = 0) + H_2(v = 0) \quad (23a)$$

$$M^+ + C_2H_6 \rightarrow MC_2H_2^+ + H_2(v = 0) + H_2(v = 1) \quad (23b)$$

its first vibrationally excited state. A tendency to eliminate excited H_2 is consistent with a mechanism involving a tight transition state for reductive elimination of H_2 for IV. A similar proposal has also been made elsewhere.[46]

For the case of Y^+, reaction with CH_3CD_3 can lead to several possible metal–ethyne complexes, reaction 24. The ratio of

$$M^+ + CH_3CD_3 \rightarrow MC_2H_2^+ + HD + D_2 \quad (24a)$$

$$M^+ + CH_3CD_3 \rightarrow MC_2HD^+ + 2HD \quad (24b)$$

$$M^+ + CH_3CD_3 \rightarrow MC_2D_2^+ + HD + H_2 \quad (24c)$$

$YC_2H_2^+$ to YC_2HD^+ to $YC_2D_2^+$ observed is approximately 1:5:4 in the low-energy feature and 1:10:1 in the high-energy feature. The reaction with M = Sc shows ratios of 1:4–5:1 in the low-energy feature and 1:10:1 in the high-energy feature. A statistical distribution of products would show a ratio of 1:4:1. The deviation from the statistical ratio for M = Y at low energy may be due to slight differences in the energetics of reaction 24; reaction 24b is 0.065 eV more endothermic than reaction 24c, while reaction 24a is 0.037 eV more endothermic. However, the 1:5:4 ratio holds up to 0.5 eV. It is surprising that the ratio does not become more statistical with energy. The high-energy feature for M = Sc and Y is consistent with preferential 1,2-dehydrogenation without scrambling.

MH_2^+. In contrast to all other first-row transition metals, Sc^+ efficiently forms products with two covalently bound ligands in reactions with hydrocarbons under single-collision conditions. In particular, ScH_2^+ is formed in reaction with ethane.[11,12] The most straightforward mechanism for production of MH_2^+ is decomposition of intermediate IV by loss of C_2H_4, Scheme I. In reaction with CH_3CD_3, $ScHD^+$ is formed almost exclusively, supporting this mechanism.[47] This means that reaction 8 competes directly with reactions 11 and 12, which are much more energetically favorable. Nevertheless, this endothermic process is dominant for some energy range for Y^+, La^+, and Lu^+. This result has been attributed to the relative phase space of these processes and to angular momentum considerations. Since reaction 8 is a bond fission reaction, it should have a loose transition state and thus a high density of states. In contrast, reactions 11 and 12 are reductive eliminations that should involve fairly tight transition states and therefore lower state densities. The angular momentum conservation arguments require a somewhat more involved explanation, which has been discussed previously.[11] Basically, it is easier to conserve angular momentum if the reduced mass of the products is large. This factor favors reaction 8 (reduced mass = 21.4, 23.4, and 24.2 amu for Y^+, La^+, and Lu^+, respectively) over reaction 12 (reduced mass = 2.0 amu for Y^+, La^+, and Lu^+).

All of these group 3 ions have only two valence electrons. Since one metal electron is needed for each covalent M^+–H bond, no valence electrons are available to bond to the C_2H_4 in intermediate IV. This bond is thus only a dative bond; i.e., the electrons in the ethene π bond are donated into an accepting orbital on the metal, and the metal has no available d electrons with which to back-bond into the π^* orbital of the ethene. Metals to the right in the periodic table have electrons for back-bonding such that the $(H)_2M^+$–C_2H_4 bond strength increases. This makes MH_2^+ formation energetically unfavorable in comparison to $MC_2H_4^+$ formation.

At $\simeq$2 eV for Sc^+, Y^+, and La^+ and $\simeq$3 eV for Lu^+, the cross section for MH_2^+ begins to decline. Two processes could account for this behavior. First, MH_2^+ can decompose to $M^+ + H_2$ beginning at 1.41 eV, the energy necessary to dehydrogenate ethane, Table IV. The fact that the cross section decline is delayed from this thermodynamic onset suggests that excess energy is tied up in translation and in internal modes of the C_2H_4 product. This is similar to the behavior of MH^+ formed in these reactions and in the reactions with methane. While this decomposition could take place at higher energies, an alternative explanation for the

(45) Sunderlin, L. S.; Armentrout, P. B., submitted for publication in *Int. J. Mass Spectrom. Ion Processes.*

(46) Beauchamp, J. L.; Stevens, A. E.; Corderman, R. R. *Pure Appl. Chem.* **1979**, *51*, 967–978.

(47) No definitive results concerning this product could be obtained for the reaction of Y^+ with CH_3CD_3 due to mass resolution restrictions.

decline in the MH_2^+ cross section is competition with another process. The peaks in these cross sections correlate well with the onset of MH^+ production, about 2 eV for Sc^+, Y^+, and La^+ and 2.5 eV for Lu^+. This observation can be taken as evidence that MH^+ and MH_2^+ are formed via a common intermediate, II. Since MH^+ formation is a bond fission while MH_2^+ production requires a rearrangement, formation of MH^+ could rapidly deplete the population of intermediate II even though it is the more endothermic pathway.

Summary

The reaction of Sc^+, Y^+, La^+, and Lu^+ with methane results in MCH_2^+ at low energy, with MH^+ and a small amount of MCH_3^+ formed at higher energies. With ethane, $MC_2H_4^+$ and $MC_2H_2^+$ are formed exothermically for M = Sc, Y, and La and endothermically for M = Lu. Endothermic channels for all four ions include MH_2^+ at low energies and MH^+, MCH_3^+, and MCH_2^+ at elevated energies. The thermochemistry of these various product ions is derived from analysis of the reaction thresholds. The bond energies (given in Table V) indicate single bonds to H and CH_3 and double bonds to CH_2. The values are generally consistent with an "intrinsic bond energy" model corrected for the electronic excitation needed for promotion to an orbital suitable for bonding.

The experimental results of both systems are interpreted to indicate that most of the reactivity is due to an insertive mechanism but that, with methane, some fraction of the MH^+ is due to a more direct process. The amount of insertive reaction relative to direct reaction increases down the third column from Sc^+ to Y^+ to La^+, with Lu^+ being more direct than the other elements. Qualitative molecular orbital arguments previously shown to be useful in describing the reaction of metal ions with H_2 and CH_4 are consistent with the results seen. There is an apparent bottleneck in the pathway to reach the ground-state insertion products H-M^+-CH_3 and H-M^+-C_2H_5 for the most highly populated states of Sc^+, Y^+, and La^+. This is attributed to a surface crossing between the triplet surfaces of the reactants and the singlet surfaces of the intermediates.

Consistent with earlier results for Sc^+ with ethane, Y^+ and apparently La^+ dehydrogenate ethane by two mechanisms: 1,2-dehydrogenation to form M^+-ethane at low energy and 1,1-dehydrogenation to form the metal-ethylidene ion at higher energy. There are also two channels for double dehydrogenation of ethane by Sc^+, Y^+, and La^+. The data for all three elements are similar and are consistent with either of two mechanisms: one involving different electronic states of the intermediates formed and one where vibrationally excited H_2 is eliminated. For Lu^+ there is only one apparent channel for both reactions.

Overall, the reactivities of the group 3 metal ions with methane and ethane are quite similar. Futher, the thermochemistry of the metal hydride ions, metal dihydride ions, metal methyl ions, and metal methylidene ions for Sc^+, Y^+, and La^+ are all comparable. Lu^+ differs somewhat in both respects. The difference between La^+ (which has no 4f electrons) and Lu^+ (which has a filled 4f shell) must be a result of the differing 4f orbital occupancy. However, there is no indication of direct participation of the 4f orbitals. Rather the effect of the 4f orbitals is probably an indirect one. Namely, the occupation of these orbitals raises the energy of the 5d shell such that the two valence electrons in the ground state of Lu^+ both occupy the 6s orbital. In La^+, the energy of the 5d and 6s orbitals is much closer, leading to open shell electron configurations. The closed-shell stability of the $Lu^+(^1S,6s^2)$ ground state probably accounts for its distinct reactivity compared with Sc^+, Y^+, and La^+.

Acknowledgment. This research is funded by National Science Foundation Grant No. 8796289. L.S.S. thanks the NSF for a predoctoral fellowship.

High-Resolution Absorption and Luminescence Spectroscopy of a Cyclometalated Rhodium(III) Complex: $[Rh(phpy)_2(bpy)]^+$

Arne Zilian, Urs Maeder,† Alex von Zelewski,† and Hans U. Güdel*

Contribution from the Institut für Anorganische und Physikalische Chemie, Universität Bern, Freiestrasse 3, 3000 Bern 9, Switzerland. *Received October 31, 1988*

Abstract: The title complex was prepared in crystalline form as the Cl^- and PF_6^- salt and studied by absorption and luminescence spectroscopy down to 5 K. The highly resolved crystal spectra of the PF_6^- salt allow the location of four electronic origins for the lowest energy transitions: 22 030 (A), 22 078 (B), 22 128 (C), and 22 150 cm^{-1} (D). The rich fine structure in the absorption spectrum between 22 000 and 26 000 cm^{-1} is fully interpreted as vibrational sideband structure on the origins C and D. The sharp structure of the low-temperature luminescence spectrum, which is built on the origin A, is distinctly different. In terms of the usual classification, the transitions C and D are assigned as singlet-triplet (RhLCT) charge-transfer transitions. The transitions A and B, exhibiting some properties typical of ligand-centered singlet-triplet excitations but also some significant deviations, are more difficult to classify.

1. Introduction

The study of the lowest energy excited states in chelate complexes of $4d^6$ and $5d^6$ metal ions continues to attract a great deal of attention. Complexes with a broad range of photophysical and photochemical properties have been synthesized by chemical variation of the ligands and the metal ion.[1-3] Measurements of absorption and luminescence spectra in solutions and glasses at room and liquid-nitrogen temperature are usually combined with a study of the quantum yield and decay behavior of luminescence to characterize new complexes.

Inhomogeneous broadening of absorption and emission lines in glassy matrices is often very pronounced, thus seriously reducing their information content. Nonexponential luminescence decay behavior originating from a distribution of different sites in the sample is frequently observed in such environments. Many glasses have properties depending on their history, which seriously limits

* Author to whom correspondence is addressed.
† Institut de Chimie Minérale, Université de Fribourg Pérolles, 1700 Fribourg, Switzerland.

(1) Krausz, E. R.; Ferguson, J. *Prog. Inorg. Chem.*, in press.
(2) Juris, A.; Barigeletti, F.; Campagna, S.; Balzani, V.; Belser, P.; von Zelewsky, A. *Coord. Chem. Rev.* **1988**, *84*, 85.
(3) Lees, A. J. *Chem. Rev.* **1987**, *87*, 711.

0002-7863/89/1511-3855$01.50/0